DOI: 10.32615/ps.2019.131 PHOTOSYNTHETICA 58 (SI): 194-204, 2020

Special issue in honour of Prof. Reto J. Strasser

Plant biomass in salt-stressed young maize plants can be modelled with photosynthetic performance

V. GALIĆ[*], M. MAZUR[*,+], D. ŠIMIĆ[*], Z. ZDUNIĆ[*], and M. FRANIĆ[**]

Agricultural Institute Osijek, Department of Maize Breeding and Genetics, Južno predgrađe 17, 31000 Osijek, Croatia[*]
Institute of Agriculture and Tourism, Department of Agriculture and Nutrition, Karla Huguesa 8, 52440 Poreč, Croatia[**]

Abstract

Predicting responses to stressful conditions is very important. Chlorophyll *a* fluorescence (ChlF) can be used to assess effects of various stresses on photosynthetic performance. We tested the responses of five 10-d old maize hybrids to salinity stress by measuring ChlF parameters, fresh (FM) and dry mass (DM). ChlF data were incorporated into a penalized regression model to predict biomass traits. The values of FM and DM significantly decreased under salt stress by 42 and 25%, respectively. Strong responses in ChlF parameters assessing the absorption dissipation and trapping fluxes to NaCl treatment were detected. In penalized regression models, 118 transients showed greater (R^2 = 0.663 for FM and R^2 = 0.678 for DM), although comparable, predictive abilities as 18 selected JIP-test parameters (R^2 = 0.597 for FM and R^2 = 0.636 for DM). Genetic assessment of developed models is needed, as they efficiently predict biomass traits and provide physiological context to the obtained predictions.

Additional key words: biomass predictions; NaCl stress; partial least squares regression; performance index; photosystem II.

Introduction

Maize (*Zea mays* L.) is one of three most important cereal crops used as a human food, feed for livestock, and raw material in many industries. Abiotic stress is one of the main causes of yield loss worldwide and soil salinity is very common abiotic factor in the crop production which negatively affects plant growth at multiple stages in the form of both hyperosmotic and hyperionic stresses (Munns 2002, James *et al.* 2011, Gupta and Huang 2014, Kan *et al.* 2017). In general, maize is considered moderately sensitive to salt stress (Zörb *et al.* 2004, Farooq *et al.* 2015), a category which comprises plants that maintain growth in saline soils with an electrical conductivity between 3 and 6 dS m^{-1} (Hasanuzzaman *et al.* 2013). A saline level of more than 0.25 M NaCl may inhibit maize growth and cause severe wilting (Menezes-Benavente *et al.* 2004). Moderate soil salinity in the range of 8 to 10 dS m^{-1} results in yield losses up to 55% in maize (Satir and Berberoglu 2016). As the salinity increases, growth decreases until plants become chlorotic and die (Dikilitas and Karakas 2010). A saline soil can be defined as the one with electrical conductivity of the saturation extract in the root zone exceeding 4 dS m^{-1} at 25°C with exchangeable sodium of 15%, which approximates 40 mM NaCl (Shrivastava and Kumar 2015). Different factors, such as long drought periods, high surface

Received 9 May 2019, *accepted* 23 September 2019.
+Corresponding author; e-mail: maja.mazur@poljinos.hr
Abbreviations: ABS/RC – absorption per active reaction center; Area – complementary area above the fluorescence induction curve; ChlF – chlorophyll *a* fluorescence; CGM – crop growth model; DI_0/RC – dissipation per active reaction center; DM – dry mass; ET_0/RC – electron transport per active reaction center; F_0 – minimal fluorescence intensity; F_M – maximal fluorescence intensity; F_V – maximal variable fluorescence; G2P – genotype-to-phenotype; PC – principal component; PCA – principal component analysis; PI_{ABS} – performance index on absorption basis; PI_{total} – performance index (potential) for energy conservation from photons absorbed by PSII to the reduction of PSI end acceptors; PLS – partial least squares (regression); RC – reaction center; RC/ABS – Q_A-reducing RCs per PSII antenna chlorophyll; RE_0/RC – electron flux reducing the end electron acceptors at the PSI acceptor side per reaction center; RMSEP – root mean square error of prediction; ROS – reactive oxygen species; S_m – normalized complementary area above the fluorescence induction curve; SNP – single nucleotide polymorphisms; T_{FM} – time needed to reach F_M; TR_0/RC – trapping per active reaction center; δ_{Ro} – efficiency/probability with which an electron from the intersystem electron carriers transferred to reduce end acceptors at the PSI acceptor side; φ_{Eo} – quantum yield of electron transport; φ_{Po} – maximum quantum yield of primary photochemistry; φ_{Ro} – quantum yield for reduction of end electron acceptors at the PSI acceptor side; ψ_{Eo} – efficiency/probability that an electron moves further than Q_A^-.
This manuscript is for the Special Issue on 'JIP-test in chlorophyll fluorescence and photosynthesis research' in honour of Professor Reto J. Strasser.

evaporation, using saline water for irrigation, excessive use of water in dry climates with heavy soils, and practice of waterlogging without adequate drainage, lead to soil salinization (Mateo-Sagasta and Burke 2011, Tomescu *et al.* 2017). According to FAO, estimates around 800 million hectares of land worldwide is affected by either salinity (397 million ha) or sodicity (434 million ha) (FAO 2005) which accounts for more than 6% of the world's total land area (Munns 2005).

Soil salinity causes accumulation of toxic Na^+ and Cl^- concentrations in plant tissues (Munns 2002) which is particularly damaging during germination and at the early stages of growth (Park *et al.* 2016). Exposure to NaCl induces hyperosmotic and hyperionic stress and an ion toxicity (particularly caused by Cl^-) when plants are exposed to high concentrations of this salt for long periods (Kalaji and Pietkiewicz 1993, Munns 2002, Chaves *et al.* 2009). The accumulation of Na^+ and Cl^- in the cells causes ion imbalance and excess uptake might cause significant physiological disorders (Gupta and Huang 2014). At the plant level, salt stress can reduce growth in an early phase of plant development which significantly reduces the yield (Zörb *et al.* 2018). At the cellular level, a high Na^+ concentration inhibits uptake of K^+ ions, which is an essential element for growth and development, resulting in reduced productivity or even death (James *et al.* 2011). High concentrations of Na^+ in the soil cause hyperosmotic stress due to a rapid change in the osmotic potential between the plant and the environment which reduces water absorption capacity of plants (Munns 2002, Fricke *et al.* 2006, Schleiff 2008) triggering plant responses similar to drought stress (Kalaji *et al.* 2018). At high salinity levels, salts accumulate in leaf tissues to excessive concentrations. Salts may accumulate in the apoplast and dehydrate the cell, they may accumulate in the cytoplasm inhibiting enzymes involved in carbohydrate metabolism, or they may accumulate in the chloroplast and exert a direct toxic effect on photosynthetic processes (Munns and Tester 2008). At the initial stage of salinity stress, osmotic stress causes changes in various physiological processes, such as decreased photosynthetic efficiency of both photosystems, PSI and PSII (Liska *et al*. 2004, Stepien and Klobus 2006, Qu *et al.* 2012, Gao *et al*. 2016), although photochemical activity of PSII in maize is more sensitive to salt stress than that of PSI (Kan *et al.* 2017). The effects of salt stress have been already investigated by the measurements of ChlF emitted by plants. ChlF measurements are informative in assessment of structure and function of the photosynthetic apparatus (Strasser *et al.* 2010) and the JIP-test (Strasser *et al.* 2000) has become widely used for large-scale screening of stress effects (Kalaji *et al.* 2016). The JIP-test was proven to be a very useful tool for the *in vivo* investigations of the adaptive behavior of the photosynthetic apparatus to a wide variety of stressors, as it translates the shape changes of the O-J-I-P transient curve to quantitative changes of the several parameters (Strasser *et al*. 2004) and provides assessment of the cascade of chloroplast redox reactions at microsecond or millisecond scales (Kalaji *et al.* 2016). Particularly, the JIP-test and ChlF transients have been used so far to assess the effects of salt stress in many species, such as barley (Kalaji *et al*. 2011), wheat (Mehta *et al*. 2010), sunflower (Umar *et al*. 2019), maize (Kan *et al*. 2017), *Tilia cordata* Mill. (Kalaji *et al*. 2018), sorghum (Sayyad-Amin *et al*. 2016, Zhang *et al*. 2018), and rocket (Hniličková *et al*. 2017).

With the advent of the mass availability of the genotyping data, such as single nucleotide polymorphisms (SNP) from genotyping diversity arrays or sequencing efforts, the crop genomic prediction models were developed (*i.e.*, genomic/genome-wide selection models). The next step towards obtaining more accurate predictions would be the integration of the new phenotypes that are easy to measure, highly heritable, and correlated with traits of interest into the models. Subsequently, these relevant variables have to be integrated into the genotype-to-phenotype (G2P) models to improve the model prediction accuracy (van Eeuwijk *et al*. 2018). Technow *et al*. (2015) developed a crop growth model (CGM), which integrates the physiological variables into the genome-wide prediction models. The aim of CGMs is not only to increase prediction accuracy, but also to provide the biological framework in plant breeding to increase the understanding of plant adaptation to environments and stresses (Cooper *et al*. 2016, Messina *et al*. 2018). Since ChlF kinetics is highly informative tool used for studying effects of different environmental stresses, including salt stress on photosynthesis (Kalaji *et al.* 2011), it might serve as a new, adequate high-throughput phenotyping tool in CGM and G2P models, especially, because some ChlF parameters are affected by similar genetic regions as grain yield in stressful environments (Galić *et al*. 2019).

Here, we provided a first step towards the use of ChlF data in prediction models by incorporating the measured transients and calculated parameters into a penalized regression model aiming to predict biomass responses in terms of FM and DM to salinity. Additionally, the photosynthetic responses of young plants of five maize hybrids to salinity stress were analyzed by the means of biomass accumulation and JIP-test.

Materials and methods

Plant material and experimental design: The experiments were carried out with five commercial maize (*Zea mays* L.) hybrids of Agricultural Institute Osijek, Croatia. Hybrids were chosen in a way to represent the maturity variations frequently observed in the farmers' fields in South-Eastern Europe. Hybrid pedigrees, FAO maturity classifications, and parental components with their respective genetic backgrounds were:

Hybrid	FAO maturity	♀ parent	♀ background	♂ parent	♂ background
378	370	OS 2340-8	Iodent	OS 27488	Oh43
444	450	OS 3-48	Iodent	OS 135-88	Lancaster
505	510	OS 23-48	Iodent	OS 942	Oh43
Drava	420	OS 84-28A	Iodent	OS 942	Oh43
Veli	590	OS 024445	Iodent	OS KLT14	Stiff Stalk Synthetic

Experiments were set under controlled conditions with temperature of 25°C, 16/8-h day/night regime, and light intensity of 200 μmol(photon) m^{-2} s^{-1}. Soil properties were 70 mg(NH_3 + NO_3^-) L^{-1}, 80 mg(P_2O_5) L^{-1}, 90 mg(K_2O) L^{-1}, 70% organic matter, and pH = 5.7 ($CaCl_3$). Seeds of the five maize hybrids were planted in trays filled with organic soil substrate in two treatments (control and NaCl) and four replicates. Briefly, 15 seeds of each hybrid planted in each tray for each genotype in both control and NaCl treatment were considered a single biological replicate (totally eight trays per genotype). Soil for the NaCl treatment was treated with dilution of 50 mM of NaCl per kilogram of soil. The mentioned concentration was chosen according to the results by Yang and Lu (2005) as the middle concentration which affects the PSII and is feasible to find in field-growing scenarios. Plantlets were grown for 10 d and watered with spray bottle every second day before the ChlF measurements.

ChlF measurements and weighting: ChlF was measured with hand-held fluorimeter *Handy-PEA* (*Hansatech*, King's Lynn, UK) in the middle of the first fully developed leaf. In each replicate of each treatment ten uniformly developed plants were measured, comprising totally 40 measurements per genotype per treatment. After the dark adaptation of 30 min, ChlF transients were induced by a red light saturation pulse [650 nm; 3,200 mmol m^{-2} s^{-1}] on the leaf surface exposed by the leaf clip (12.56 mm^2). The light pulse induces ChlF increase from minimal fluorescence (F_0), when all reaction centers are open, to maximal fluorescence (F_M), when all reaction centers are closed. During the 1-s measurement, 118 data points are collected. ChlF data were processed with *PEA Plus* software *(V1.10)* provided with the fluorimeter. The JIP-test (Strasser and Strasser 1995, Strasser *et al.* 2000, 2004) was used to analyze each ChlF transient. JIP-test is a mathematical model based on the theory of 'energy flow' across thylakoid membranes (Strasser *et al.* 2000) developed as a biophysical tool for assessment of the cascade of chloroplast redox reactions at microsecond or millisecond scales (Kalaji *et al.* 2016). The formulas in Appendix illustrate how each of the mentioned biophysical parameters can be calculated from the original fluorescence measurements. JIP-test data were used to perform principal component analysis (PCA). Parameters for further analyses and statistical modelling were chosen according to the series of the PCAs to represent best the variation existing among hybrids and their reactions to salinity.

Aboveground biomass of each measured plant was weighed on the four decimal laboratory scale and designated as FM. Plants were oven dried for 24 h in an open 15-ml falcon tube at 80°C before weighting for DM. DM was expressed as percentage of FM.

Statistical analyses and model validation: All statistical analyses were carried out in *R* programming environment (*R Core Team* 2018). Analysis of variance and the post-hoc tests were performed in package *agricolae* (Mendiburu and Simon 2015) after *Shapiro-Wilk*'s test of normality. According to the *p* values from *Shapiro-Wilk*'s test, it was chosen between ordinary least-squares-based *Fisher*'s LSD test and *Kruskal-Wallis* test for multiple comparisons. Analysis of variance was performed with mean values of replicates (trays), n = 40. For PCA, the *R* base function *prcomp* was used with log-transformed centered variables. The plots were constructed with the *ggbiplot2* library (Vu 2011). Only the components explaining more than 10% of the variance were analyzed. Only parameters with correlation coefficients < 0.9 were analyzed in this manner.

Partial least squares (PLS) regression was used to fit the models between the ChlF and biomass-related data (FM, DM). PLS regression was chosen because the method was designed to effectively solve the collinearity problem often present among sequential measurements and multiple predictor variables in the regression models. The models were fitted with *pls* library (Mevik *et al*. 2018) function *plsr*. After the model fitting, model calibration was carried out with 10-fold cross validation procedure. Namely, in this procedure, the data set was divided into ten equal subsets, and the data from nine subsets were used to predict a single subset, after which the correlation between the predicted and observed values of the dependent variable was calculated. The process was repeated (folded) until the last single set was predicted. Mean correlation across the folds was calculated in each step as the independent variables were rearranged in all possible manners reducing their dimensionality while explaining the highest possible proportion of variance in both x and y directions. After the cross-validation procedure, the number of components (dimensions) was chosen according to the absolute lowest calculated value of the root mean square error of prediction (RMSEP). The model with absolute lowest value of RMSEP was considered a calibrated model. The dependent variables in the models were FM and DM and two models per trait were constructed: first with the selected 18 JIP-test parameters used for PCA chosen to represent best the variation in the dataset, and second with all 118 measured ChlF transients as independent variables (predictors).

For further (independent) validation of the models, we planted another independent experiment similar to the control from the first experiment. The calculated models for predicting FM and DM were employed and the correlations between the observed and predicted values were calculated, as well as the RMSEP values of the predictions.

Results

Effects of NaCl stress on selected ChlF and JIP-test parameters are shown in Fig. 1. Values of parameters were normalized to their respective controls in order to compare genotypes. Significant differences were detected between genotypes in control and NaCl treatment for all examined parameters and both biomass-related traits. Effect of NaCl treatment was significant for both biomass-related traits and most ChlF parameters. Values of time to reach F_M (T_{FM}), electron transport per active reaction center (ET_0/RC), φ_{Po}, and φ_{Ro} did not show significant changes under the NaCl stress (Table 1S, *supplement*).

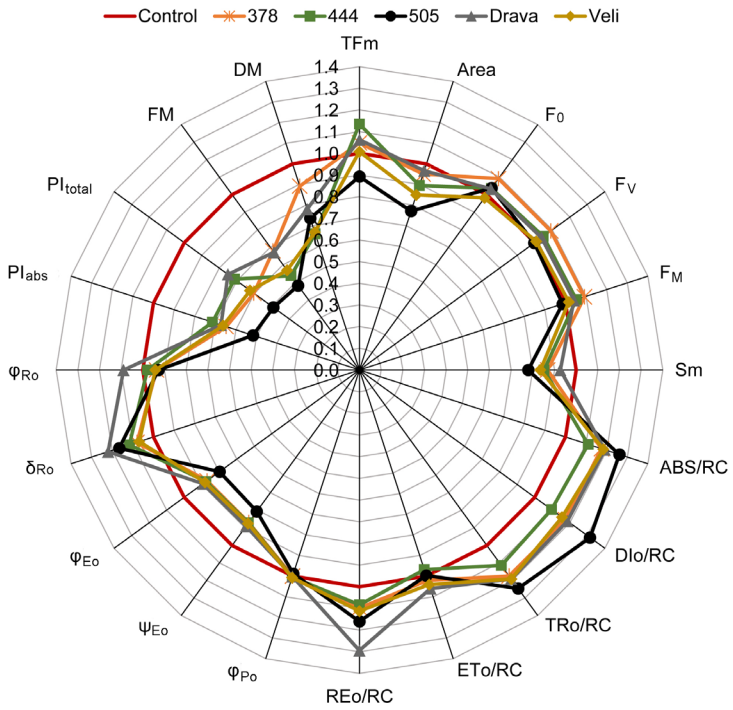

Fig. 1. Changes in JIP-test (for definitions, formulas, and abbreviations *see* Appendix) and biomass parameters induced by salinity in five maize hybrids. Values represent the means (n = 40). Significant differences between NaCl treatment and control at α=0.05 level were detected for all parameters except T_{FM}, ET_0/RC, φ_{Po}, and φ_{Ro}. Significant differences between genotypes at α=0.05 level were detected in control and NaCl treatment for all examined parameters. Full list of values and statistics is available in Table 1S.

Data extracted from the recorded fluorescence transient: Values of total complementary area between the fluorescence induction curve and F_M (Area) and normalized complementary area above the fluorescence induction curve (S_m) decreased in NaCl treatment in all investigated genotypes. The largest decrease in both parameters was recorded in genotype 505, while genotype Drava showed the lowest decrease. Drava, 378, and 444 values of F_0, F_M, and F_V parameters increased under the NaCl stress (Fig. 1).

Specific fluxes per active reaction center: Values of absorption (ABS/RC), dissipation (DI_0/RC), trapping (TR_0/RC) per active reaction center (RC), and electron flux reducing the end electron acceptors at the PSI acceptor side per RC (RE_0/RC) increased under the NaCl treatment in all investigated genotypes. The lowest increase was recorded in genotype 444, while genotype 505 showed the largest increase in ABS/RC, DI_0/RC, and TR_0/RC, while the genotype Drava showed the largest increase in RE_0/RC in relation to their respective controls (Fig. 1).

Quantum yields and efficiencies/probabilities: Values of maximum quantum yield of PSII (φ_{Po}) and quantum yield for reduction of end electron acceptors at the PSI acceptor side (φ_{Ro}) did not change significantly under the NaCl treatment. In contrast, efficiency/probability that an electron moves further than Q_A^- (ψ_{Eo}) and quantum yield of electron transport (φ_{Eo}) decreased while efficiency/probability with which an electron from the intersystem electron carriers is transferred to reduce end electron acceptors at the PSI acceptor side (δ_{Ro}) increased in NaCl treatment. Genotype 505 showed the largest decrease in ψ_{Eo} and φ_{Eo} compared with the control, while decrease in values of these parameters in other genotypes was similar. The largest increase in δ_{Ro} was found in genotype Drava and the smallest in genotype Veli (Fig. 1).

Performance indexes: Significant effect of NaCl treatment was recorded for both PI_{ABS} and PI_{total}. In stressed plants, PI_{ABS} values were considerably lower than that in nonstressed plants. The largest deviation from the control was recorded for genotype 505, while the smallest deviation was recorded for genotype 444. Similarly, under the NaCl stress, PI_{total} values showed the highest drop in genotype 505, while the smallest decrease was recorded in Drava genotype (Fig. 1).

Biomass-related traits: Under the NaCl stress, the values of FM and DM significantly decreased. Genotype 505 showed the largest decrease of FM, while the lowest decrease was recorded in genotypes 378 and Drava. Genotype 378 also showed the smallest decrease of DM, while the largest deviation from the control was recorded in genotypes 444 and Veli (Fig. 1).

Principal component analysis: The PCA explained 76.6% of the variance (Fig. 2) in the data in the first two principal components (PCs). Inspection of the biplot (Fig. 2) and Table 1 showed that PC1 is mainly correlated with φ_{Ro}, φ_{Po}, and PI_{total} in positive direction and F_0 in negative direction. The PC2 is mostly described with DM and FM in positive direction and δ_{Ro} in negative direction. The genotype-treatment combinations formed two distinct groups: control and NaCl along the PC2, although there were also interesting differences between genotypes within NaCl treatment and control. Namely, hybrid Veli was separated from other hybrids along PC1 in both treatments. The individual scores of other hybrids in the biplot showed an

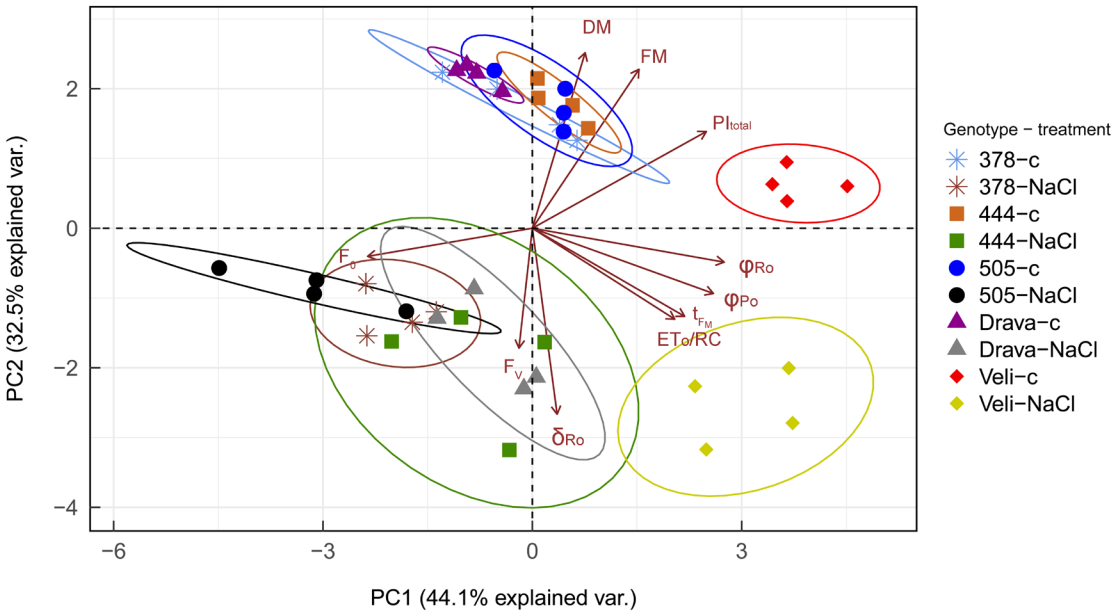

Fig. 2. Principal component analysis of variation among reactions of five maize hybrids to elevated contents of soil NaCl. Arrows represent the eigenvalues of each of the eight selected chlorophyll *a* fluorescence parameters (for definitions, formulas, and abbreviations *see* Appendix) with correlation coefficients < 0.9, fresh mass (FM) and dry mass (DM). Ellipses around the groups are the calculated 95% confidence intervals. c – control; NaCl – 40 mM NaCl soil treatment; PC – principal component.

Table 1. Loading weights, communalities, and eigenvalues from principal component analysis of JIP-test (for definitions, formulas, and abbreviations *see* Appendix) and biomass parameters for first two principal components (PC). FM – fresh mass, DM – dry mass.

Parameter	Loading		Communality	
	PC1	PC2	PC1	PC2
T_{FM}	0.354	–0.238	0.743	–0.430
F_0	–0.383	–0.076	–0.803	–0.137
F_M	–0.031	–0.324	–0.065	–0.584
ET_0/RC	0.331	–0.246	0.694	–0.443
φ_{Po}	0.420	–0.176	0.883	–0.318
δ_{Ro}	0.058	–0.503	0.121	–0.907
φ_{Ro}	0.445	–0.092	0.935	–0.165
PI_{total}	0.404	0.262	0.848	0.472
FM [mg]	0.248	0.430	0.520	0.775
DM [% FM]	0.123	0.475	0.257	0.856
Eigenvalue	4.407	3.248	-	-

overlapping pattern, especially in the control, positioning them around the origin of the PC1 and on the positive side of PC2. Grouping of variants was similar in the NaCl treatment with hybrids 444 and Drava positioned around the origin of PC1 and on the negative side of PC2 and hybrids 378 and 505 positioned in the negative quadrant in both PCs showing the largest decrease in performance. The drop in performance was mostly visible through the increase in F_0 and dissipation per RC and decrease in performance indexes and biomass traits.

Model predicting the plant biomass traits from ChlF data: The PLS models predicting the young plant FM and DM were set to examine the usability of ChlF data in abiotic stress quantification and to test the predictive potential of the data. First two models were set with 18 biophysical parameters of JIP-test (Appendix), some of which were also used for PCA, as independent variables (x) and FM and DM as dependent variables (y). The models explained 59.7% of the variance for FM (Fig. 3*A*) and 63.6% of variance for DM (Fig. 3*B*) with low RMSEP indicating fairly high precision of the predictions. The other two models were set with all 118 ChlF transient data points measured through the initial 1 s upon illumination with saturating pulse of light as independent variables. The models explained 66.3% of the variance for FM (Fig. 3*A*) and 67.8% variance for DM (Fig. 3*B*) with lower but comparable values of RMSEP indicating comparable predictive abilities as the models using JIP-test parameters as independent variables. Generally, transients showed greater but comparable prediction accuracy for both examined traits.

Predictive abilities of the models were further tested in an independent scenario which was a replicate of the control experiment. Correlation coefficients between predicted and observed values were lower compared to initial estimates, and ranged from 0.496 to 0.641 (Table 2).

The highest loadings in models with JIP-test parameters as independent variables and FM as dependent variable were observed for PI_{total} and δ_{Ro}, followed by fluxes per RC, while near-zero loadings were assigned to the data extracted from recorded transients (Fig. 4*A*, Appendix). In a model with DM as dependent variable and JIP-test parameters as independent variables, the largest loading weight was observed for quantum yield of electron transport, followed by maximum quantum yield of PSII,

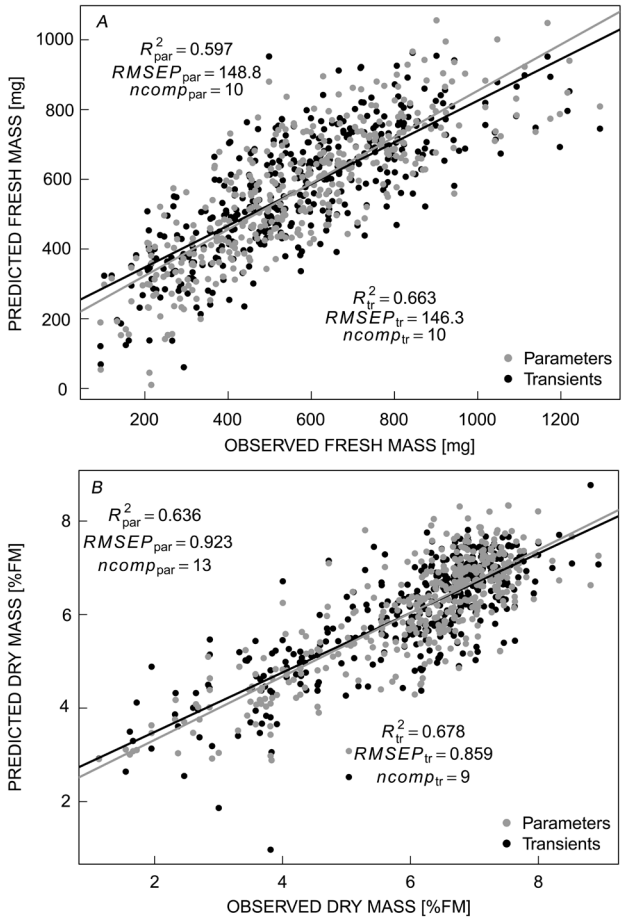

Fig. 3. Scatterplots of the partial least squares (PLS) regression model with fresh mass per plant [mg] as dependent variable (*A*), dry mass [% FM] as dependent variable (*B*), and 18 chlorophyll *a* fluorescence parameters/118 chlorophyll *a* fluorescence transients as predictors. Coefficients of determination (R^2), root mean squares of prediction (RMSEP), and number of components used for prediction (ncomp) are shown for models calibrated using the 10-fold cross validation. Both R^2 values are significant at α=0.001, n = 400. FM – fresh mass.

electron transport, and electron flux reducing the end electron acceptors at PSI side per active RC (Fig. 4*C*). In models with transient data as independent variables for both FM and DM as dependent variables, the most pronounced loading weights (both positive and negative) were observed in the transient areas corresponding to J-I and P parts of the O-J-I-P band (Fig. 4*B*,*D*).

Discussion

Salt stress is manifested in two ways: as osmotic stress causing dehydration and ionic stress causing ionic imbalance. Both effects, osmotic and ionic, affect the photosynthesis process and many factors can lead to the decrease in photosynthetic performance under the salt stress. Namely, Na^+ ions, which enter the maize cells, inhibit the development, increase the reactive oxygen species (ROS) production, result in decrease of stomatal conductance, *etc*. Consequently, these metabolic alterations reflect in photosynthetic performance (Farooq *et al*. 2015). The physiological response in maize is expected to be genotype specific, as there is a variation present in everything from Na^+ ion uptake and accumulation to expression of the genes included in antioxidative response and protein synthesis (Soares *et al*. 2018). The parameter φ_{Po} is often used to express the physiological condition of a plant, but proved to be very stable under some stressful conditions, especially osmotic stress (Shabala *et al.* 1998, Kocheva *et al.* 2004, Deng *et al.* 2010, Akram *et al*. 2011), corroborated with reduced water absorption capacity of plants under the NaCl stress (Fricke *et al.* 2006, Schleiff 2008). Stable values of φ_{Po} under the salt stress in our study indicate that NaCl treatment did not irreversibly damage PSII functioning, as the values were kept above critical levels (Woo *et al*. 2011). Other ChlF parameters, giving information on the heterogeneity of electron transport, PSII RCs, and overall photosynthetic performance showed significant effects of the NaCl stress along with both biomass-related traits.

Lowest reduction in biomass parameters, FM and DM, observed in hybrids Drava and 378 compared to their respective controls might indicate higher tolerance to salt stress. Accumulation of DM is an excellent indicator of stress tolerance and changes relative to control conditions can be used to discriminate cultivars that are tolerant to osmotic stress from the susceptible ones (Chen *et al.* 2016). Fresh biomass partitioning to water and dry matter is affected by salt stress in such way that the maintenance of the water fraction cannot be maintained, inducing the reduction of leaf expansion, thus lowering the amount of photosynthetic tissues (Sultana *et al.* 1999, Negrão *et al*. 2017). Drop in FM in our study was more pronounced than the drop in DM possibly indicating lowering in relative water content due to the NaCl-induced osmotic stress (Živčák *et al*. 2008).

Significant changes in biophysical parameters suggest that increased NaCl concentration alters the PSII RC density, which can be seen from the increase in ABS/RC values. Similar increases under the NaCl-stressed wheat leaves have been reported by Mehta *et al.* (2010). Increase in ABS/RC indicated inhibition of electron transport from Q_A^- to Q_B, and transformation of RCs to 'silent' RCs (Yusuf *et al.* 2010). Increase in dissipation energy (DI_0/RC) supports the change in RC functionality, as the increase in dissipation could indicate that some of the RCs have transformed to 'heat sinks' to dissipate excess energy (Strasser *et al.* 2000). This is usually accompanied with decrease of Q_A-reducing RCs per PSII antenna chlorophyll (RC/ABS). This is also in concordance with decreases in φ_{Eo} under the NaCl stress, which corresponds to a decrease in the efficiency of electron transport to the intersystem electron acceptors (Strasser *et al.* 2010). Increase in ABS/RC during drought stress is usually accompanied by increased trapped energy flux (TR_0/RC) (Christen *et al.* 2007). Kalaji *et al*. (2018) showed that in terms of distinguishing two types of stress affecting osmotic status of the plant drought and salinity, absorption, trapping, and dissipation energy fluxes show similar patterns of reactions, making them indistinguishable by the means

Table 2. Number of components used for predictions (ncomp), root mean square of prediction (RMSEP), and the correlations between the predicted and observed values (*R*) for the validation of the partial least squares (PLS) models with independent data set. All correlation coefficients are significantly different from zero at α=0.001, *n* (independent data set) = 200. FM – fresh mass.

Trait	Model	ncomp	RMSEP [mg]	RMSEP [%]	*R*
Fresh mass [mg]	Parameters	10	147.8	-	0.512
	Transients	10	126.2	-	0.641
Dry mass [% FM]	Parameters	13	-	1.97	0.496
	Transients	9	-	2.20	0.528

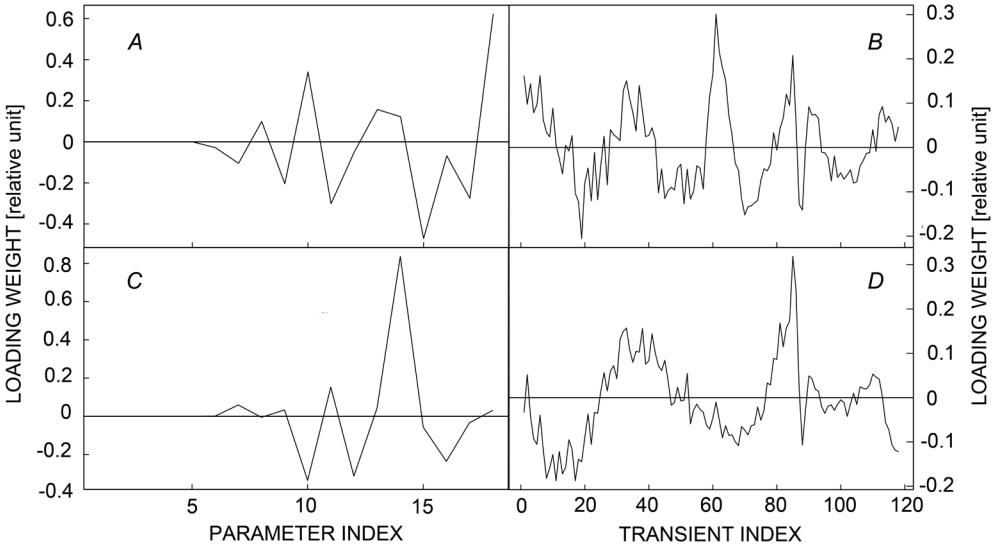

Fig. 4. Loading weights of calibrated models with fresh mass [mg] as dependent and 18 selected ChlF parameters as independent variables (*A*), fresh mass [mg] as dependent and 118 ChlF transients as independent variables (*B*), dry mass [% FM] as dependent and 18 selected ChlF parameters as independent variables (*C*), and dry mass [% FM] as dependent and 118 ChlF transients as independent variables (*D*).

of ChlF. The patterns observed in their study were also confirmed in this present study, indicating the dissociation of the light-harvesting complex from the PSII and the loss of energy connectivity. Salt stress did not influence the number of quanta absorbed per unit of time (based on changes in φ_{Po}), but it did cause a decrease in the efficiency of forward electron transport (ψ_{Eo}). Similar relations of φ_{Po} and ψ_{Eo} were also presented by Mehta *et al.* (2010). Concomitantly, values of PI_{ABS} decreased under the NaCl stress since φ_{Po} and ψ_{Eo} are used in the calculation of PI_{ABS} (along with RC/ABS, which also decreased under the NaCl stress). The decrease in the performance index under the salt stress has been previously presented for various plant species (Mehta *et al.* 2010, Kalaji *et al.* 2011, 2018; Kan *et al*. 2017, Zhang *et al*. 2018). Decreasing trends of PI_{ABS} and PI_{total} were caused by the decrease in ψ_{Eo} and increase in absorption flux representing lower number of RCs reducing Q_A per PSII antenna chlorophyll. Lowest decrease in performance in NaCl treatment recorded in 444 was due to the lower increase in absorption flux accompanied by the lowest increase in dissipation per active RC and moderate decrease in ψ_{Eo}. The lowest decrease in PI_{total} recorded in hybrid Drava was, on the other hand, caused by the near mean decrease in ψ_{Eo}, but largest increase in efficiency of reduction of end electron acceptors on PSI side (δ_{Ro}). Similar decreases of PI_{ABS} and PI_{total} were obtained by Zhang *et al.* (2018). Increase of δ_{Ro} in the NaCl treatment is probably due to decrease in redox balance of PSII electron acceptors due to lower PSII activity. Furthermore, increased values of δ_{Ro} might be associated with higher resilience of PSI to salt stress compared to PSII (Umar *et al*. 2019).

As there were evident differences in responses of different cultivars in our study (Fig. 1), we aimed to test the relative importance of each variable to the clustering of five maize genotypes by the means of PCA. The results obtained in PCA indicate that the grouping of cultivars might have been caused by the differences in their respective genetic backgrounds. The maternal line of hybrid Veli is of the same origin as the B73 line from the study by Soares *et al*. (2018). B73 was found to be among the more tolerant cultivars to the salt stress, as was the case in our study with hybrid Veli, rightmost positioned on PC1 axis in the PCA in both control and NaCl treatment (Fig. 1). The separation of hybrids along PC1 was mostly determined by quantum yields of primary photochemistry and reduction of end electron acceptors on PSI side, F_0, time to reach F_M, and electron transport per RC. A reason for hybrid

Veli positioning on the positive side of PC1 might be its later maturity and unrelated pedigree compared to other hybrids examined in this study. The positions along PC2 of the respective controls of every hybrid were mostly defined by higher values of biomass traits and higher PI_{total}. Contrarily, plants in NaCl treatment showed higher δ_{Ro} representing higher tolerance of PSI to salt stress than PSII (Umar *et al*. 2019).

According to the differences detected in both ChlF and biomass traits and the eigenvalues of biomass and complex correlation structure of traits ChlF, the predictive ability of ChlF data was tested by designing the penalized PLS models with raw transients and the selected JIP-test parameters as predictors and biomass traits (FM, DM) as response variables. Aims to develop predictive models with ChlF data were reported before in predictions of lemon fruit quality (Nedbal *et al*. 2000), relative water content of drought stressed *Phaseolus vulgaris* cv. Cheren Starozagorski (Goltsev *et al.* 2012), growth of *Lactuca sativa* L. seedlings (Moriyuki and Fukuda 2016), mortality from drought in various species (Guadagno *et al*. 2017), and physiological dynamics of *Acer platanoides* (Artherton *et al.* 2016).

The absolute highest loading weight in model with FM as response and JIP-test parameters as predictors obtained for PI_{total} (Fig. 4*A*) was in accordance with the index complexity. The PI_{total} is an index containing the inference about several key photosynthetic processes from dissipation, absorbance, and quantum yield of primary photochemistry to the probability that electron from the intersystem carrier reduces the end electron acceptor on PSI side (Strasser *et al*. 2010, Appendix). Value of performance indexes in assessment of plant biomass accumulation was also confirmed in study of Sayyad-Amin *et al*. (2016). Other important variable in model aiming to predict response in FM was parameter δ_{Ro}, indicating the importance of PSI functionality in young plant formation (Brestič *et al*. 2015). Moreover, the higher salt stress tolerance of PSI implying the increase in efficiency with which an electron from the intersystem electron carriers is transferred to reduce end electron acceptors at the PSI electron acceptor side would provide the biological relevance to the obtained loading weights as PSI functioning is very important in salt stress tolerance (Yamori and Shikanai 2016). Near-zero loadings assigned to the data extracted from O-J-I-P transient curve were caused by better representation of the relationships of certain parts of the transient curve by the calculated parameters and multiparametric expressions. The inspection of loading weights for model with DM as response (Fig. 4*C*) and JIP-test parameters as predictors indicated that quantum yield of electron transport, followed by maximum quantum yield of PSII, electron transport, and electron flux reducing the end electron acceptors at PSI side per active RC best explain the variation in JIP-test parameters linked to DM. Moreover, the higher loading values for quantum yield of electron transport, maximum quantum yield of PSII, electron transport, and electron flux reducing the end electron acceptors at PSI side per active RC indicate that finer differences might have been captured with these parameters compared to multivariate expressions such as performance indexes. The same parameters were shown to be important in predictions of relative water content in beans using artificial neural networks (Goltsev *et al*. 2012) indicating their importance in various species in context of biomass prediction in osmotic stress conditions. The small differences in prediction accuracies obtained between the models indicate the robustness of the biophysical interpretation of transients and efficient extraction of information from the fluorescence transient OJIP curve. Expectedly, performance indexes as complex and sensitive indicators of plant status (Stirbet and Govindjee 2011) were shown to contribute the most in describing growth of young maize plants in terms of FM. The loading weights in models with transients as predictor variables varied according to the plateaus of the O-J-I-P curve induction dynamics with peaks in J-I part in model with FM as response, and I-P in model with DM as response (Fig. 4*B*,*D*). Despite the small absolute difference in predictive abilities of the models using biophysical expressions compared to raw transients, the use of transients might be a better option in the modelling approach where ultimate goal is explained variance, as there are no discernable differences in the computation process with smaller or larger number of variables. The composite variables are created in the PLS models and more variance explained presents comparative advantage. However, in the CGMs and models that appeal to human interpretation, the biophysical parameters such as performance indexes and their components provide physiological framework to the predictions while explaining a fair proportion of variance.

The predictive ability of the model was confirmed through the validation with independent data set (Table 2) although with lower accuracy than in cross-validation. Cause of the lower accuracies of predictions obtained is probably the lower amount of variation present in this set, as it is actually a reproduction of the control experiment.

All hybrids examined in this study showed significant reactions to salinity stress in terms of photosynthetic performance and biomass traits. Hybrids 378 and Drava showed the lowest decrease in biomass traits compared to their respective controls which was accompanied in Drava by the highest values of PI_{total} and with increase in data extracted from fluorescence transient in 378. The similarity in responses of these two hybrids might be caused by the related pedigrees, as parental lines of these two hybrids are from same heterotic groups. The distinct reaction of hybrid Veli detected in PCA was probably due to its later maturity and distinct pedigree compared to other examined hybrids. Selected JIP-test parameters showed lower but comparable predictive abilities of FM and DM in regression models, although more information was captured when raw transients were used. As ChlF represents the method capable of detection of various stresses (Kalaji *et al*. 2016), with biophysical interpretation and physiological explanations (Strasser *et al.* 2000, 2004, 2010) and high heritability of the obtained parameters (Šimić *et al*. 2014) it can be used as phenotype in CGM and G2P models, although higher number of the progenies

need to be tested and further assessment is needed with special emphasis on quantitative genetic approach to test the structure of variance in the obtained predictions and ability to predict various phenotypes. However, models using ChlF data shown in this study represent good guideline in further research, as they describe fair proportions of variance in examined phenotypes, show predictive ability in independent scenario, and are contextualized in a biological framework provided by biophysical interpretation and physiological relevance of ChlF parameters.

References

Akram M., Ashraf M.Y., Jamil M. *et al*.: Nitrogen application improves gas exchange characteristics and chlorophyll fluorescence in maize hybrids under salinity conditions. – Russ. J. Plant Physl+ **58**: 394-401, 2011.

Artherton J., Nichol C.J., Porcar-Castell A.: Using spectral chlorophyll fluorescence and the photochemical reflectance index to predict physiological dynamics. – Remote Sens. Environ. **176**: 17-30, 2016.

Brestič M., Živčák M., Kunderlíková K. *et al*.: Low PSI content limits the photoprotection of PSI and PSII in early growth stages of chlorophyll *b*-deficient wheat mutant lines. – Photosynth. Res. **125**: 151-166, 2015.

Chaves M.M., Flexas J., Pinheiro C.: Photosynthesis under drought and salt stress: Regulation mechanisms from whole plant to cell. – Ann. Bot.-London **103**: 551-560, 2009.

Chen D., Wang S., Cao B.: Genotypic variation in growth and physiological response to drought stress and re-watering reveals the critical role of recovery in drought adaptation in maize seedlings. – Front. Plant Sci. **6**: 1214, 2016.

Christen D., Schönmann S., Jermini M. *et al*.: Characterization and early detection of grapevine (*Vitis vinifera*) stress responses to esca disease by *in situ* chlorophyll fluorescence and comparison with drought stress. – Environ. Exp. Bot. **60**: 504-514, 2007.

Cooper M., Technow F., Messina C. *et al*.: Use of crop growth models with whole-genome prediction: application to a maize multienvironment trial. – Crop Sci. **56**: 2141-2156, 2016.

Deng C.N., Zhang G.X., Pan X.L., Zhao K.Y.: Chlorophyll fluorescence and gas exchange responses of maize seedlings to saline-alkaline stress. – Bulg. J. Agric. Sci. **16**: 49-58, 2010.

Dikilitas M., Karakas S.: Salts as potential environmental pollutants, their types, effects on plants and approaches for their phytoremediation. – In: Ashraf M., Ozturk, M., Ahmad M.S.A. (ed.): Plant Adaptation and Phytoremediation. Pp. 357-381. Springer, New York 2010.

FAO: Global network on integrated soil management for sustainable use of salt-affected soils. FAO Land and Plant Nutrition Management Service, Rome 2005. http://www.fao.org/soils-portal/soil-management/management-of-some-problem-soils/salt-affected-soils/more-information-on-salt-affected-soils/en/ (*Accessed* 4 November 2019)

Farooq M., Hussain M., Wakeel A., Siddique K.H.M.: Salt stress in maize: effects, resistance mechanisms, and management. A review. – Agron. Sustain. Dev. **35**: 461-481, 2015.

Fricke W., Akhiyarova G., Wei W. *et al.*: The short-term growth response to salt of the developing barley leaf. – J. Exp. Bot. **57**: 1079-1095, 2006.

Galić V., Franić M., Jambrović A. *et al.*: Genetic correlations between photosynthetic and yield performance in maize are different under two heat scenarios during flowering. – Front. Plant Sci. **10**: 566, 2019.

Gao Y., Lu Y., Wu M.Q. *et al.*: Ability to remove Na^+ and retain K^+ correlates with salt tolerance in two maize inbred lines seedlings. – Front. Plant Sci. **7**: e0116697, 2016.

Goltsev V., Zaharieva I., Chernev P. *et al.*: Drought-induced modifications of photosynthetic electron transport in intact leaves: Analysis and use of neural networks as a tool for a rapid non-invasive estimation. – BBA-Bioenergetics **1817**: 1490-1498, 2012.

Guadagno C.R., Ewers B.E., Speckman H.N. *et al*.: Dead or alive? Using membrane failure and chlorophyll *a* fluorescence to predict plant mortality from drought. – Plant Physiol. **175**: 223-234, 2017.

Gupta B., Huang B.: Mechanism of salinity tolerance in plants: Physiological, biochemical, and molecular characterization. – Int. J. Genomics **2014**: 701596, 2014.

Hasanuzzaman M., Nahar K., Fujita M. *et al*.: Enhancing plant productivity under salt stress: relevance of poly-omics. – In: Ahmad P., Azooz M.M., Prasad M.N.V. (ed.): Salt Stress in Plants: Signalling, Omics and Adaptations. Pp. 113-156. Springer, New York 2013.

Hniličková H., Hnilička F., Martinková J., Kraus K.: Effects of salt stress on water status, photosynthesis and chlorophyll fluorescence of rocket. – Plant Soil Environ. **63**: 362-367, 2017.

James R.A., Blake C., Byrt C.S., Munns R.: Major genes for Na^+ exclusion, *Nax1* and *Nax2* (wheat *HKT1;4* and *HKT1;5*), decrease Na^+ accumulation in bread wheat leaves under saline and waterlogged conditions. – J. Exp. Bot. **62**: 2939-2947, 2011.

Kalaji H.M., Govindjee, Bosa K. *et al*.: Effects of salt stress on photosystem II efficiency and CO_2 assimilation of two Syrian barley landraces. – Environ. Exp. Bot. **73**: 64-72, 2011.

Kalaji H.M., Jajoo A., Oukarroum A. *et al*.: Chlorophyll *a* fluorescence as a tool to monitor physiological status of plants under abiotic stress conditions. – Acta Physiol. Plant. **38**: 102, 2016.

Kalaji H.M., Pietkiewicz S.: Salinity effects on plant growth and other physiological processes. – Acta Physiol. Plant. **15**: 89-124, 1993.

Kalaji H.M., Račková L., Paganová V. *et al*.: Can chlorophyll-*a* fluorescence parameters be used as bio-indicators to distinguish between drought and salinity stress in *Tilia cordata* Mill? – Environ. Exp. Bot. **152**: 149-157, 2018.

Kan X., Ren J., Chen T. *et al.*: Effects of salinity on photosynthesis in maize probed by prompt fluorescence, delayed fluorescence and P700 signals. – Environ. Exp. Bot. **140**: 56-64, 2017.

Kocheva K., Lambrev P., Georgiev G. *et al*.: Evaluation of chlorophyll fluorescence and membrane injury in the leaves of barley cultivars under osmotic stress. – Bioelectrochemistry **63**: 121-124, 2004.

Liska A.J., Shevchenko A., Pick U., Katz A.: Enhanced photosynthesis and redox energy production contribute to salinity tolerance in *Dunaliella* as revealed by homology-based proteomics. – Plant Physiol. **136**: 2806-2817, 2004.

Mateo-Sagasta J., Burke J.: Agriculture and Water Quality Interactions: A Global Overview. – SOLAW Background Thematic Report – TR08. Pp. 46. FAO, Rome 2011.

Mehta P., Jajoo A., Mathur S., Bharti S.: Chlorophyll *a* fluorescence study revealing effects of high salt stress on Photosystem II in wheat leaves. – Plant Physiol. Bioch. **48**: 16-20, 2010.

Mendiburu F., Simon R.: Agricolae – Ten years of an open source statistical tool for experiments in breeding, agriculture and biology. – PeerJ PrePrints **3**: e1404v1, 2015.

Menezes-Benavente L., Kernodle S.P., Margis-Pinheiro M., Scandalios J.G.: Salt-induced antioxidant metabolism defenses in maize (*Zea mays* L.) seedlings. – Redox Rep. **9**: 29-36, 2004.

Messina C.D., Technow F., Tang T. *et al*.: Leveraging biological insight and environmental variation to improve phenotypic prediction: Integrating crop growth models (CGM) with whole genome prediction (WGP). – Eur. J. Agron. **100**: 151-162, 2018.

Mevik B.-H., Wehrens R., Liland K.H.: pls: Partial least squares and principal component regression. R package version 2.7-0, 2018. *Available at*: https://CRAN.R-project.org/package=pls (*Accessed* 3 May 2019)

Moriyuki S., Fukuda H.: High-throughput growth prediction for *Lactuca sativa* L. seedlings using chlorophyll fluorescence in a plant factory with artificial lighting. – Front. Plant Sci. **7**: 394, 2016.

Munns R.: Comparative physiology of salt and water stress. – Plant Cell Environ. **25**: 239-250, 2002.

Munns R.: Genes and salt tolerance: bringing them together. – New Phytol. **167**: 645-663, 2005.

Munns R., Tester M.: Mechanisms of salinity tolerance. – Annu. Rev. Plant Biol. **59**: 651-681, 2008.

Nedbal L., Soukupová J., Whitmarsh J., Trtílek M.: Postharvest imaging of chlorophyll fluorescence from lemons can be used to predict fruit quality. – Photosynthetica **38**: 571-579, 2000.

Negrão S., Schmöckel S.M., Tester M.: Evaluating physiological responses of plants to salinity stress. – Ann. Bot.-London **119**: 1-11, 2017.

Park H.J., Kim W.Y., Yun D.J.: A new insight of salt stress signaling in plant. – Mol. Cell **39**: 447-459, 2016.

Qu C.X., Liu C., Gong X.L. *et al*.: Impairment of maize seedling photosynthesis caused by a combination of potassium deficiency and salt stress. – Environ. Exp. Bot. **75**: 134-141, 2012.

R Core Team: R: A language and environment for statistical computing. R Foundation for Statistical Computing, Vienna 2018. *Available at*: https://www.R-project.org/

Satir O., Berberoglu S.: Crop yield prediction under soil salinity using satellite derived vegetation indices. – Field Crop. Res. **192**: 134-143, 2016.

Sayyad-Amin P., Jahansooz M.R., Borzouei A., Ajili F.: Changes in photosynthetic pigments and chlorophyll-*a* fluorescence attributes of sweet-forage and grain sorghum cultivars under salt stress. – J. Biol. Phys. **42**: 601-620, 2016.

Schleiff U.: Analysis of water supply of plants under saline soil conditions and conclusions for research on crop salt tolerance. – J. Agron. Crop Sci. **194**: 1-8, 2008.

Shabala S.N., Shabala S.I., Martynenko A.I. *et al*.: Salinity effect on bioelectric activity, growth, Na^+ accumulation and chlorophyll fluorescence of maize leaves: A comparative survey and prospects for screening. – Aust. J. Plant Physiol. **25**: 609-616, 1998.

Shrivastava P., Kumar R.: Soil salinity: A serious environmental issue and plant growth promoting bacteria as one of the tools for its alleviation. – Saudi J. Biol. Sci. **22**: 123-131, 2015.

Soares A.L.C., Geilfus C.M., Carpentier S.C.: Genotype-specific growth and proteomic responses of maize toward salt stress. – Front. Plant Sci. **9**: 661, 2018.

Stepien P., Klobus G.: Water relations and photosynthesis in *Cucumis sativus* L. leaves under salt stress. – Biol. Plantarum **50**: 610-616, 2006.

Stirbet A., Govindjee: On the relation between the Kautsky effect (chlorophyll *a* fluorescence induction) and Photosystem II: Basics and applications of the OJIP fluorescence transient. – J. Photoch. Photobio. B **104**: 236-257, 2011.

Strasser B.J., Strasser R.J.: Measuring fast fluorescence tran-sients to address environmental questions: The JIP test. – In: Mathis P. (ed.): Photosynthesis: From Light to Biosphere. Vol. 5. Pp. 977-980. Kluwer Academic Publishers, Dordrecht 1995.

Strasser R.J., Srivastava A., Tsimilli-Michael M.: The fluorescence transient as a tool to characterize and screen photosynthetic samples. – In: Yunus M., Pathre U., Mohanty P. (ed.): Probing Photosynthesis: Mechanism, Regulation and Adaptation. Pp. 445-483. CRC Press, New York 2000.

Strasser R.J., Tsimilli-Michael M., Qiang S., Goltsev V.: Simultaneous *in vivo* recording of prompt and delayed fluorescence and 820-nm reflection changes during drying and after rehydration of the resurrection plant *Haberlea rhodopensis*. – BBA-Bioenergetics **1797**: 1313-1326, 2010.

Strasser R.J., Tsimilli-Michael M., Srivastava A.: Analysis of the chlorophyll *a* fluorescence transient. – In: Papageorgiou G.C., Govindjee (ed.): Chlorophyll *a* Fluorescence: A Signature of Photosynthesis. Advances in Photosynthesis and Respiration. Pp. 321-362. Springer, Dordrecht 2004.

Sultana N., Ikeda T., Itoh R.: Effect of NaCl salinity on photosynthesis and dry matter accumulation in developing rice grains. – Environ. Exp. Bot. **42**: 211-220, 1999.

Šimić D., Lepeduš H., Jurković V. *et al*.: Quantitative genetic analysis of chlorophyll *a* fluorescence parameters in maize in the field environments. – J. Integr. Plant Biol. **56**: 695-708, 2014.

Technow F., Messina C.D., Totir L.R., Cooper M.: integrating crop growth models with whole genome prediction through approximate Bayesian computation. – PLoS ONE **10**: e0130855, 2015.

Tomescu D., Şumălan R., Copolovici L., Copolovici D.: The influence of soil salinity on volatile organic compounds emission and photosynthetic parameters of *Solanum lycopersicum* L. varieties. – Open Life Sci. **12**: 135-142, 2017.

Umar M., Uddin Z., Siddiqui Z.S.: Responses of photosynthetic apparatus in sunflower cultivars to combined drought and salt stress. – Photosynthetica **57**: 627-639, 2019.

van Eeuwijk F.A., Bustos-Korts D., Millet E.J. *et al.*: Modelling strategies for assessing and increasing the effectiveness of new phenotyping techniques in plant breeding. – Plant Sci. **282**: 23-39, 2018.

Vu V.: ggbiplot: A ggplot2 based biplot. R package version 0.55, 2011.

Woo N., Badger M.R., Pogson B.J.: A rapid, non-invasive procedure for quantitative assessment of drought survival using chlorophyll fluorescence. – In: Stewart P., Globig S. (ed.): Photosynthesis: Genetic, Environmental and Evolutionary Aspects. Pp. 266-288. Apple Academic Press, Oakville 2011.

Yamori W., Shikanai T.: Physiological functions of cyclic electron transport around photosystem i in sustaining photosynthesis and plant growth. – Annu. Rev. Plant Biol. **67**: 81-106, 2016.

Yang X., Lu C.: Photosynthesis is improved by exogenous glycinebetaine in salt-stressed maize plants. – Physiol. Plantarum **124**: 343-352, 2005.

Yusuf M.A., Kumar D., Rajwanshi R. *et al*.: Overexpression of γ-tocopherol methyl transferase gene in transgenic *Brassica juncea* plants alleviates abiotic stress: Physiological and chlorophyll *a* fluorescence measurements. – BBA-Bioenergetics **1797**: 1428-1438, 2010.

Zhang H., Xu N., Wu X. *et al*.: Effects of four types of sodium salt stress on plant growth and photosynthetic apparatus in sorghum leaves. – J. Plant Interact. **13**: 506-513, 2018.

Zörb C., Schmitt S., Neeb A. *et al*.: The biochemical reaction of maize (*Zea mays* L.) to salt stress is characterized by a mitigation of symptoms and not by a specific adaptation. – Plant Sci. **167**: 91-100, 2004.

Zörb C., Geilfus C.M., Dietz K.J.: Salinity and crop yield. – Plant Biol. **21**: 31-38, 2018.

Živčák M., Brestič M., Olšovská K., Slamka P.: Performance index as a sensitive indicator of water stress in *Triticum aestivum* L. – Plant Soil Environ. **54**: 133-139, 2008.

Appendix. Definition of terms and formulae of JIP-test parameters and expressions modified from Strasser *et al.* (2010).

Parameter	Parameter index	Description
		Data extracted from the recorded fluorescence transient
T_{FM}	1	Time needed to reach F_M
Area	2	Complementary area above the fluorescence induction curve
F_0	3	Minimal fluorescence intensity [all PSII reaction centers (RCs) are open]
F_M	4	Maximal fluorescence intensity (all PSII RCs are closed)
F_V	5	Maximal variable fluorescence; $F_V = F_M - F_0$
S_m	6	Normalized complementary area above the fluorescence induction curve; $S_m = Area/(F_M - F_0)$
		Specific fluxes per active RC
ABS/RC	7	Absorption per active RC; $ABS/RC = M_0 \times (1/V_J) \times [1/(F_V/F_M)]$ = reciprocal of RC/ABS
DI_0/RC	8	Dissipation per active RC; $DI_0/RC = (ABS/RC) - (TR_0/RC)$
TR_0/RC	9	Trapping per active RC; $TR_0/RC = M_0 \times (1/V_J)$
ET_0/RC	10	Electron transport per active RC; $ET_0/RC = M_0 \times (1/V_J) \times (1 - V_J)$
RE_0/RC	11	Electron flux reducing the end electron acceptors at the PSI acceptor side per RC; $RE_0/RC = M_0 \times (1/V_J) \times (1 - V_I)$
		Quantum yields and efficiencies/probabilities
φ_{Po}	12	Maximum quantum yield of PSII; $\varphi_{Po} = F_V/F_M = [1 - (F_0/F_M)]$
ψ_{Eo}	13	Efficiency/probability that an electron moves further than Q_A^-; $\psi_{Eo} = 1 - V_J$
φ_{Eo}	14	Quantum yield of electron transport; $\varphi_{Eo} = [1 - (F_0/F_M)] \times (1 - V_J)$
δ_{Ro}	15	Efficiency/probability with which an electron from the intersystem electron carriers is transferred to reduce end electron acceptors at the PSI acceptor side; $\delta_{Ro} = (1 - V_I)/(1 - V_J)$
φ_{Ro}	16	Quantum yield for reduction of end electron acceptors at the PSI acceptor side; $\varphi_{Ro} = [1 - (F_0/F_M)] \times (1 - V_I)$
		Performance indexes
PI_{ABS}	17	Performance index on absorption basis; $PI_{ABS} = (RC/ABS) \times (TR_0/DI_0) \times [ET_0/(TR_0 - ET_0)]$
PI_{total}	18	Performance index (potential) for energy conservation from photons absorbed by PSII to the reduction of PSI end acceptors; $PI_{total} = PI_{ABS} \times (\delta_{Ro}/1 - \delta_{Ro})$